Magnetic-Field Dependence of Microwave Absorption and Energy Gap in Superconducting Films*

R. H. WHITE† AND M. TINKHAM
Department of Physics, University of California, Berkeley, California
(Received 4 May 1964)

We have measured the change in absorption of microwave radiation by superconducting indium, tin, and lead films as a function of magnetic field. Experiments have been conducted on films 145–700 Å thick using 8-mm- and 4-mm-wavelength microwave radiation, primarily with the magnetic field parallel to the plane of the film, but also as a function of angle between the magnetic field and the plane of the film. We observe a second-order phase change in the magnetic field, as is to be expected for films of this thickness according to the theories of Ginzburg and Landau and of Nambu and Tuan. The angular dependence of the critical field found in our measurements is in good agreement with the theory of one of the authors, which predicts an angular dependence given by the formula $(H_c \sin\theta/H_{c\parallel})+(H_c \cos\theta/H_{c\perp})^2=1$.

We have attempted to infer the magnetic-field dependence of the effective energy gap Δ from our absorption measurements in a parallel magnetic field. This inference was made by using the calculations of Miller, based on the theory of Mattis and Bardeen. The magnetic-field dependence of Δ which we found is not in agreement with previous experiment and theory, as Δ decreases much more rapidly in low magnetic fields in our experiments, nor is it completely consistent for the two frequencies used. Thus, it appears from our experimental absorption measurements that the effect of a magnetic field on a superconducting film cannot be adequately described simply by introducing a field-dependent energy-gap parameter.

I. INTRODUCTION

PARTICULARLY since the development of the Bardeen-Cooper-Schrieffer[1] theory of superconductivity, hereafter referred to as BCS, many experiments have been interpreted in terms of a superconducting energy gap. One main purpose of the present experiments was to study the effect of a parallel magnetic field on the absorption of 8-mm and 4-mm photons in superconducting films. From this data it was hoped that inferences about the effect of the field on the energy gap could be made. Previous experiments have studied the effect of a magnetic field in other ways. In particular, there have been the thermal conductivity measurements of Morris and Tinkham,[2,3] and also the tunneling experiments of Giaever and Mergerle,[4] of Douglass,[5] and of Douglass and Meservey.[6]

The samples studied were lead, tin, and indium films. They varied in thickness from 145–700 Å and were thus sufficiently thin to exhibit a second-order phase change as a function of magnetic field, as is to be expected from previous experiments[2,3,5] as well as from the theories of Ginzburg and Landau,[7] hereafter referred to as GL, and of Nambu and Tuan.[8]

The results of these microwave absorption experiments are then used in an attempt to infer the magnetic-field dependence of an effective energy-gap parameter. This is done making the initial assumption that the effect of a magnetic field can be adequately described by a dependence of an effective energy gap on magnetic field, and using the results of the theory of the electromagnetic properties of superconductors of Mattis and Bardeen.[9] The results are then compared with the GL theory,[7] and the theory of Nambu and Tuan,[8] which predict the dependence of the order parameter or energy gap on magnetic field. The results are also compared with previous experiments.[2–6]

The other main purpose of these experiments was to study the angular dependence of the critical field. The microwave absorption at 8 mm was measured in our film samples as a function of magnetic field for various orientations of the field relative to the plane of the sample. The angular dependence of the critical field was determined from these measurements. These results have been compared with the theory of Tinkham.[10]

II. EXPERIMENTAL RESULTS

Cryostat

The cryostat consists of a conventional liquid-nitrogen–liquid-helium glass Dewar pair. The o.d. of the outer (nitrogen) Dewar is $2\frac{1}{2}$ in. and the i.d. of the inner (helium) Dewar is $1\frac{1}{4}$ in. A $\frac{1}{2}$-in.-diam thin-walled stainless steel tube containing a stainless steel K-band waveguide connects the experimental chamber, placed at the bottom of the Dewar, and the Dewar head. All removable vacuum seals in the Dewar head are made with O rings. The stainless steel tube serves as a pumping line to evacuate the experimental chamber and it

* Research supported in part by the National Science Foundation and the U. S. Office of Naval Research.
† Present address: Department of Physics, University of Singapore, Singapore, Malaysia.
[1] J. Bardeen, L. N. Cooper, and J. R. Schrieffer, Phys. Rev. 108, 1175 (1957).
[2] D. E. Morris and M. Tinkham, Phys. Rev. 134, A1154 (1964); D. E. Morris, thesis University of California, Berkeley, 1962 (unpublished).
[3] D. E. Morris and M. Tinkham, Phys. Rev. Letters 6, 600 (1961).
[4] I. Giaever and K. Megerle, Phys. Rev. 122, 1101 (1961).
[5] D. H. Douglass, Jr., Phys. Rev. Letters 7, 14 (1961).
[6] R. Meservey and D. H. Douglass, Jr., Phys. Rev. 135, A24 (1964).
[7] V. L. Ginzburg and L. D. Landau, Zh. Eksperim. i Teor. Fiz. 20, 1064 (1950).
[8] Y. Nambu and S. F. Tuan, Phys. Rev. Letters 11, 119 (1963); Phys. Rev. 133, A1 (1964).
[9] D. C. Mattis and J. Bardeen, Phys. Rev. 111, 412 (1958).
[10] M. Tinkham, Phys. Rev. 129, 2413 (1963).

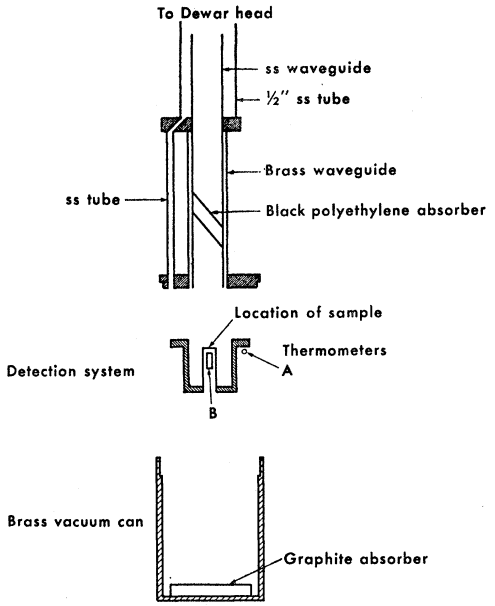

FIG. 1. The experimental chamber.

also carries the No. 40 manganin wires used as leads for the thermometers. The *K*-band waveguide is used to convey both the 8-mm and the 4-mm microwave power to the experimental chamber.

The experimental chamber is shown in Fig. 1. There is a 4-in. section of brass *K*-band waveguide inside which a $\frac{3}{8}$-in.-thick parallelepiped of black polyethylene, used as an absorber of room temperature radiation, is cemented in place with G.E. 7031 cement. This cement is used to insure that the polyethylene is maintained at the helium bath temperature. A $\frac{1}{8}$-in.-diam stainless steel tube conveys the thermometer leads over this 4-in. section.

At the lower end of the waveguide is a copper plate which serves as thermal contact between the detection system proper and the bath, and also as base plate for the brass can which is soldered to it with Wood's metal to seal the vacuum system. All the other joints in the system are silver soldered except the one between the detection system and the copper plate. This joint is held with screws, and General Cement "Silver Print" is used between the surfaces of this joint to prevent leakage of microwave radiation.

The helium bath is pumped to lower the temperature and the experiment is carried out at temperatures between the λ point (2.17°K) and 1.25°K, the lowest temperature obtainable. Temperatures higher than 1.25°K are most conveniently maintained by constricting the pumping line.

Detection of Radiation

The detection system consists of a copper flange which is used to hold the detection system to the copper base plate of the experimental chamber; a $\frac{1}{2}$-in.-diam brass tube $\frac{3}{4}$ in. long; a brass annular disk, $\frac{1}{2}$ o.d.$\times\frac{1}{8}$ in. i.d.; a $\frac{1}{8}$-in. diam stainless steel tube $\frac{1}{2}$ in. long$\times$0.005 in. wall thickness; and a 0.005$\times\frac{1}{8}$-in. diam stainless steel end cover for the stainless steel tube. These are silver soldered together as shown in Fig. 1. The sample on its substrate is cemented to the top (closed end) of the stainless steel tube with GE 7031 cement. The plane of the film is normally vertical, so that measurements can be made of the angular dependence of the critical field, but it can be mounted in the horizontal plane in order to increase microwave absorption efficiency in parallel magnetic-field measurements.

The two thermometers are nominal 470-Ω, $\frac{1}{4}$-W carbon resistors. The leads are cut short and 83% cadmium-17% zinc nonsuperconducting solder is used to attach No. 40 manganin leads. Thermometer B is cemented to the upper end of the inside of the stainless steel tube, and thermometer A is cemented to the copper flange, using GE 7031 cement.

The thin-walled, $\frac{1}{8}$-in. diam stainless steel tube serves two purposes. It is a loose thermal contact between the sample, along with thermometer B, and the bath. The thermal time constant of thermometer B (and the sample) was found to be 10 sec at 1.3°K. The stainless steel tube also serves to complete the boundary between the two sections of the experimental vacuum chamber.

The first section contains the sample on its substrate, the input waveguide, and a nonresonant microwave cavity. This part of the system is bounded by the waveguide, the copper base plate, the copper flange which is held in place with screws and sealed against radiation leakage with silver print, and the brass and stainless steel parts of the detection system.

The other section contains the thermometers. This section is bounded by the other side of the detection system, the copper base plate, a stainless steel tube for the thermometer leads, and the outer brass can.

The purpose of this separation into two sections is to prevent any microwave power striking and being absorbed in the thermometer resistors. Since the thermometers would absorb microwave power much more strongly than the sample, the experimental effect would be masked by absorption in the thermometers. Graphite is cemented to the bottom of the brass can to insure further that no microwave radiation strikes the thermometers. It was found that with a copper sample in place for test purposes the spurious magnetic-field dependence of the resistance was of the order of 0.1% or less of the usual experimental signal.

dc Bridge and Recording System

The experiment consisted of measuring the variations from balance of a dc bridge. The two low-temperature thermometers A and B formed one pair of arms

of the bridge. The other pair was formed by a 12 000-Ω wirewound resistor and a 20 000-Ω helipot. The bridge is driven by a 1.35-V mercury cell in series with about 58 000 Ω, so that the bias voltage across the two thermometers is approximately 0.4 V.

Variations from balance are measured with a Hewlett-Packard 425A microvoltmeter, and recorded on a Varian G11A strip chart recorder. Typical imbalance voltages of 1 mV (the total change in signal between zero magnetic field and $H>H_c$) are recorded. The longest time constant in the system is the thermal time constant of thermometer B, 10 sec. The thermal time constant of thermometer A is less than or equal to the time constant of the meter and recorder, 1 sec. True resistor noise, as opposed to signal fluctuations due to temperature fluctuations of the bath, is not detectable at this signal level.

The dc bridge has also been described by Morris.[2]

Microwave Apparatus

Microwave radiation of two different wavelengths, 8 and 4 mm, is used in these experiments. The 8-mm radiation is provided by an EMI R5146 reflex klystron operated at 34 Gc-sec^{-1}. This radiation is fed through various auxilliary microwave apparatus into, successively, a K_a-K-band transition, an H-plane right-angle bend, a polyethylene vacuum window, and the stainless steel waveguide of the cryostat.

The 4-mm experiments were conducted using two different sources. One source was the above-mentioned EMI 8-mm klystron and a harmonic generator, made in this laboratory, utilizing an FXR Z225S harmonic generator diode. The harmonic generator output is then fed into transition waveguide sections, the right-angle bend, and the cryostat.

For experiments with the sample mounted vertically, so that angular dependence of the critical-field measurements could be made, this source did not provide sufficient 4-mm power to produce bridge imbalance signals sufficiently greater than those due to temperature fluctuations of the bath. Therefore, for these experiments an Amperex DX 151 reflex klystron was used. Since the fundamental output of this oscillator is at 4 mm, ample power was available.

Preparation of the Film Samples

The apparatus and technique of sample preparation is essentially that described by Morris.[2] A short description is given here.

Samples were evaporated onto 22-mm square No. 1 microscope cover glasses, approximately 0.006-in. thick. The substrate is first cleaned with detergent, thoroughly rinsed, and dried in the air. It is then clamped by the corners to the bottom of a liquid-nitrogen cold trap. With only the mechanical forepump in use, a 5000-V ion bombardment voltage is applied to an aluminum electrode near the substrate. A needle valve is opened until a discharge current of 10 mA is reached. Ion bombardment cleaning of the substrate is continued for 5 min. The needle valve is closed, the ion bombardment voltage extinguished, and the chamber pumped to $3–5\times10^{-6}$ mm Hg. The upper cold trap, to which the substrate is attached, is then filled with liquid nitrogen. The pressure quickly falls to $1–2\times10^{-6}$ mm Hg, and the sample charge is evaporated.

The evaporation boats are normally 0.001-in. molybdenum strips, although 0.003-in. tantalum strips were used for the evaporation of some indium samples. The strips were approximately 2 in. long, $\frac{1}{2}$ in. wide at the ends, narrowing to $\frac{1}{4}$ in. at the middle, which is bent to form a boat for the charge. The boat is placed approximately $1\frac{1}{2}$ in. below the substrate, and the evaporation of the charge, approximately 1 mg, takes about 5 sec at the most. No close correlation between sample charge and film thickness was found, inconsistencies of the order of 50% being observed. This contradicts the experience of Morris.[2] This lack of correlation found in our experiments is due to slight modifications in the geometry between evaporations of different charges, and possibly also due to incomplete evaporation of some of the charges.

Samples are annealed at room temperature for at least one week. Any annealing of indium films longer than one week is done *in vacuo*, and all tin and lead films are annealed *in vacuo*.

Source materials of the samples are:

Metal	Purity	Source
Indium	99.999%	Indium Corp. of America
Tin	99.999%	Vulcan Detinning
Lead	99.999%	A. D. Mackay, Inc.

A portion of the sample and substrate about 1 cm $\times\frac{1}{2}$ cm is broken off for mounting in the cryostat. Samples of the proper thickness for this experiment appeared to be good mirrors in visible reflection, but visual inspection also revealed a small transmission.

III. RESULTS

Measurements

As has been noted above, the signal which is recorded in these experiments is a bridge imbalance voltage. This signal is caused by small changes in the ratio of the resistances of the two carbon resistors used as thermometers at helium temperatures. One resistor is in close thermal contact with the bath. The other resistor, thermometer B, is in relatively close thermal contact with the sample, and the sample and resistor are in relatively loose thermal contact with the bath. Thus, a small change in the temperature of the sample due to a change in the microwave power being absorbed in the sample will produce a small change in the resistance of thermometer B, linear in the change in

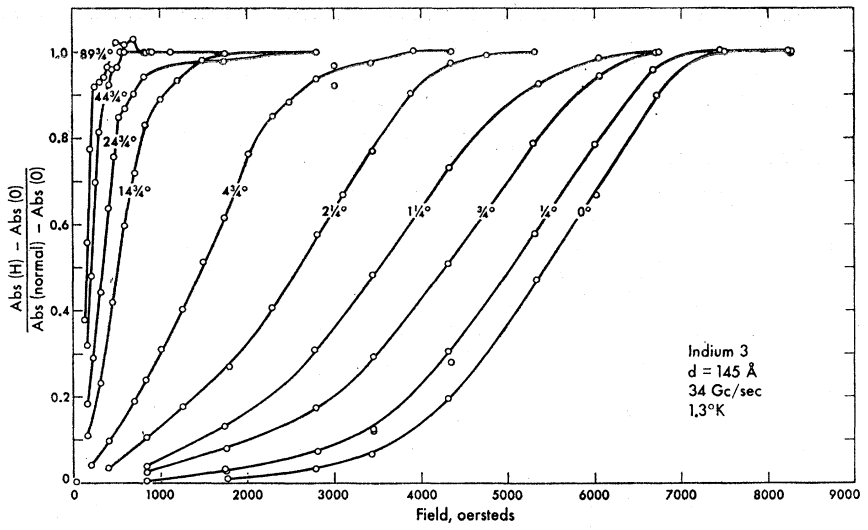

FIG. 2. Magnetic-field dependence of the absorption in sample indium 3 as a function of angle.

absorption. This, in turn, will produce a small change in the bridge imbalance voltage, again linear in the change in absorption.

Measurements have been made both at a temperature of 1.3°K and at a temperature of 2.0°K, and at microwave frequencies of 34 Gc-sec^{-1} and 68 or 71 Gc-sec^{-1}. During an experiment, a microwave source of one of these frequencies is connected to the cryostat. Sufficient microwave power is transmitted into the cryostat to produce a change in signal of the order of 1 mV between the condition $H=0$ and the condition $H=H_m>H_c$, when the sample is in the normal state. A difference in signal occurs when this microwave power is applied even in zero magnetic field. This difference is due not only to the absorption in the superconducting sample in zero magnetic field (which must be small under the experimental conditions that the photon and thermal energies are considerably less than the energy gap), but also to the absorption in the stainless steel tube which supports the substrate and thermometer B and provides their thermal contact with the bath. Since the zero magnetic-field absorption in the superconductors which we study at these frequencies and temperatures is small and can be calculated from Mattis-Bardeen[9] (see Fig. 9), and since the stainless steel absorption is unrelated to the purpose of these experiments, this zero-field absorption is subtracted out of the results presented here. The magnitude of this zero-field absorption relative to the total absorption in the maximum field (normal state) depends on frequency, temperature, and sample, and varies between 10 and 40%.

The absorption is normalized to unity at $H=H_m$, the absorption in the normal state. Thus, what is plotted in the figures giving experimental results is the difference between the absorption at magnetic field H

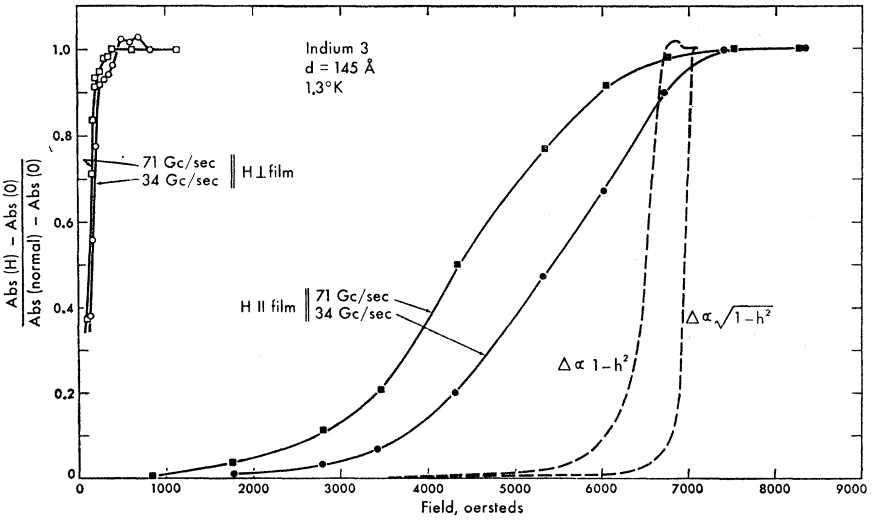

FIG. 3. Experimental magnetic-field dependence of the absorption in sample indium 3 as a function of frequency, and theoretical absorption at 34 Gc-sec^{-1} expected for field dependences of the gap of $\Delta \propto (1-h^2)$ and $(1-h^2)^{1/2}$, respectively.

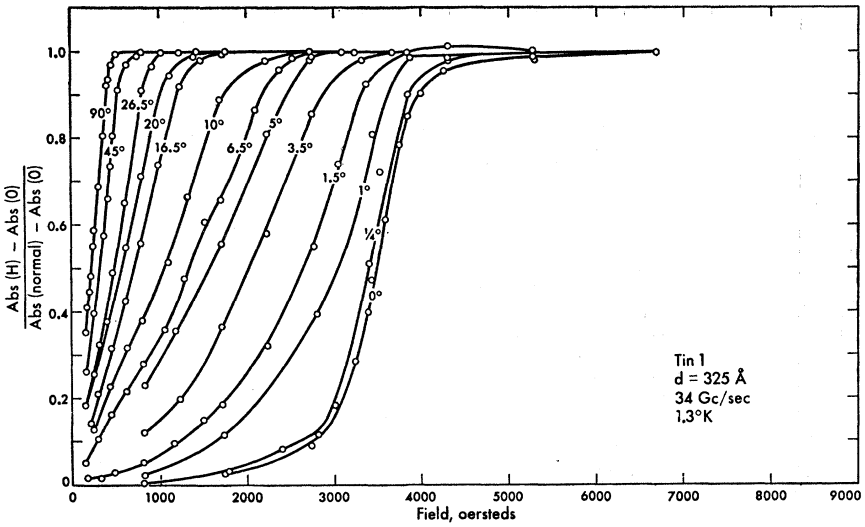

FIG. 4. Magnetic-field dependence of the absorption in sample tin 1 as a function of angle.

and the absorption at $H=0$, normalized to unity in the normal state, that is

$$\frac{\text{Absorption } (H)-\text{Absorption } (H=0)}{\text{Absorption (normal state)}-\text{Absorption } (H=0)}.$$

General Characteristics of Absorption Curves

Certain general comments can be made about the characteristics of the plots of microwave absorption versus magnetic field. These general comments are valid for all samples except one, sample indium 2, which is discussed later, although some of the general comments obtain for this sample also.

(a) One should notice in the absorption plots, Figs. 2–6, that the change in absorption is a smooth and gradual function of magnetic field. The transitions from the superconducting to the normal state are all obviously second-order transitions. This is to be expected for films of thickness such that $d<\lambda_0(5)^{1/2}$ according to the GL[7] theory, and it is in agreement with the results of Douglass[5] and of Morris.[2,3] According to calculations presented later in this article, and in agreement with crude estimates based on the weight of the charge evaporated in making the sample, this $d<\lambda_0(5)^{1/2}$ regime is the one obtained in these experiments.

(b) One may note that the absorption is always greater than or equal to the zero-field absorption, and almost always less than or equal to the normal-state absorption. The few points 1–2% greater than the normal-state absorption are probably within experimental error of the normal-state absorption.

(c) The normalized absorption at 68 or 71 Gc-sec^{-1} is always greater than or equal to the normalized absorption at 34 Gc-sec^{-1} for the same experimental conditions of sample, magnetic field, and temperature.

(d) The absorption versus field curves can be divided qualitatively into three parts for purposes of discussion:

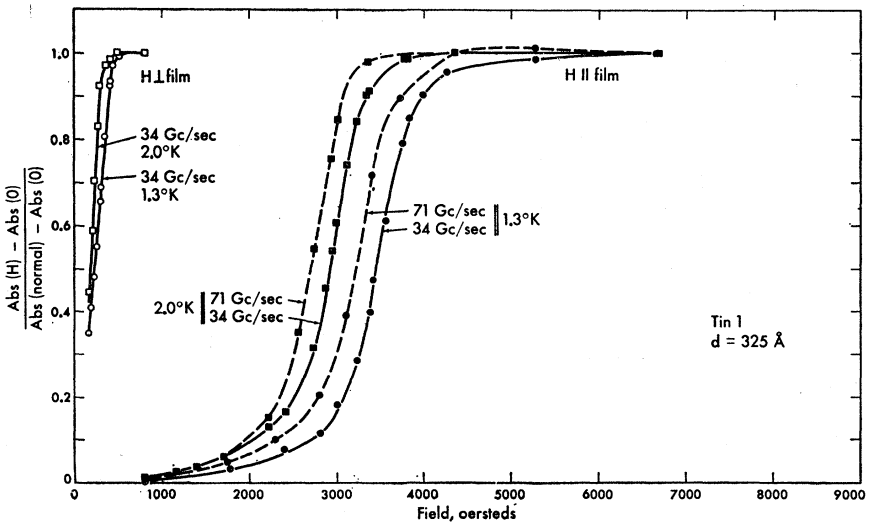

FIG. 5. Magnetic-field dependence of the absorption in sample tin 1 as a function of frequency and temperature.

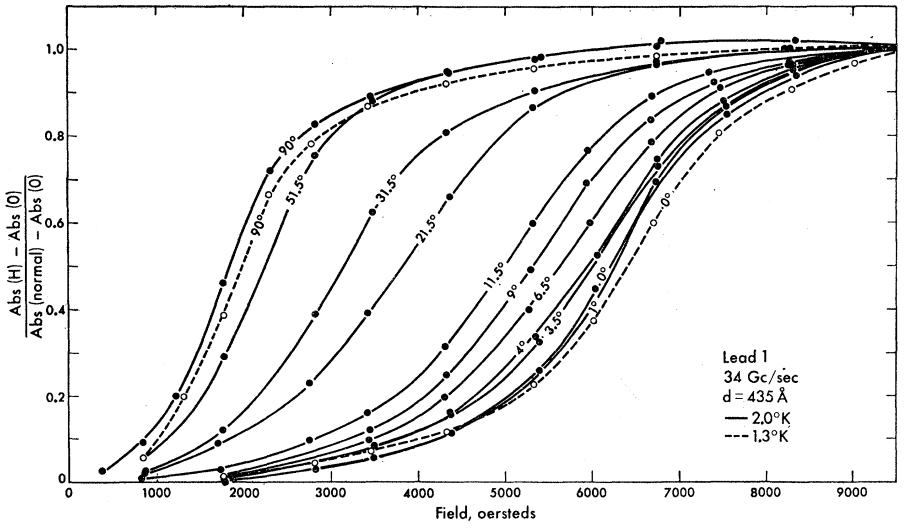

FIG. 6. Magnetic-field dependence of the absorption in sample lead 1 as a function of angle and temperature.

a portion between $H=0$ and $H\approx H_c/2$ which is approximately quadratic in H; a portion from $H\approx H_c/2$ to near the critical field which is approximately linear in H; and the rounded shoulder of the absorption curves, where the absorption approaches the normal state absorption fairly gradually.

(e) As the angle θ of the field with the plane of the film is increased from zero, the steepness of the first quadratic portion of the curve increases monotonically with θ; the second, linear portion of the curve is shifted to lower fields but the slope of this portion of the curves remains nearly unchanged as θ is increased; the final shoulder is shifted but otherwise not significantly modified.

Sample Indium 3

This is the thinnest sample which we shall discuss; $d=145$ Å. This sample was mounted vertically in the cryostat, and measurements of absorption versus magnetic field were made at various angles to the film. Figure 2 shows the absorption of 34 Gc-sec^{-1} radiation at 1.3°K plotted versus H for various angles. The condition $\theta=0$ was determined by finding the orientation with the highest critical field. It was possible to determine this orientation to within $\frac{1}{4}$ deg. A variation of $\frac{1}{8}$ deg did not produce a significant change, however.

Experiments were also conducted on this sample using 71 Gc-sec^{-1} radiation. In Fig. 3 the absorption at 1.3°K at the extreme angles $\theta=0$ and $\theta=90$ deg and for the two frequencies is shown plotted versus H.

Sample Tin 1

This tin sample is of an intermediate thickness, with $d=325$ Å. This sample was mounted vertically in the cryostat, and measurements of absorption versus angle and magnetic field were made at 34 Gc-sec^{-1} and 1.3°K. Results of these measurements are shown in Fig. 4. It was again possible to determine the orientation in which the magnetic field was parallel to the sample within $\frac{1}{4}$ degree.

Measurements were also made at 2.0°K, and at 71 Gc-sec^{-1} at both 1.3 and 2.0°K for the extreme angles. In Fig. 5 the absorption is plotted versus H at $\theta=90°$ for 34 Gc-sec^{-1} and 1.3 and 2.0°K, and also at $\theta=0$ deg for 34 and 71 Gc-sec^{-1} and 1.3 and 2.0°K.

Sample Lead 1

This sample is of thickness $d=435$ Å. It was also mounted vertically in the cryostat, and measurements of absorption versus θ and H were made at 34 Gc-sec^{-1} and 2.0°K. Also, the absorption at $\theta=0$ deg and $\theta=90$ deg was measured at 34 Gc-sec^{-1} and 1.3°K. Results of all these experiments are shown in Fig. 6.

Absorption Curves of an Anomalous Sample, Indium 2

This is the sample about which certain of the general comments made above in this section are not valid. The thickness of this sample is approximately 600 Å. This is the thickest sample which we shall discuss in detail; however, we also studied a thicker sample (Indium 1, $d\sim700$ Å) which did not exhibit the anomalous behavior described here. Sample indium 2 was mounted horizontally and a magnet which could be rotated in the horizontal plane about the cryostat was used, so that it would be possible to make measurements with the field accurately parallel to the sample. However, no systematic variation of the absorption with magnet angle was found, so a preferred orientation could not be determined. Experiments were conducted at 1.3 and 1.95°K and at 34 and 68 Gc-sec^{-1}. Absorption versus H curves are shown in Fig. 7. In order to avoid further confusion in this figure, no ex-

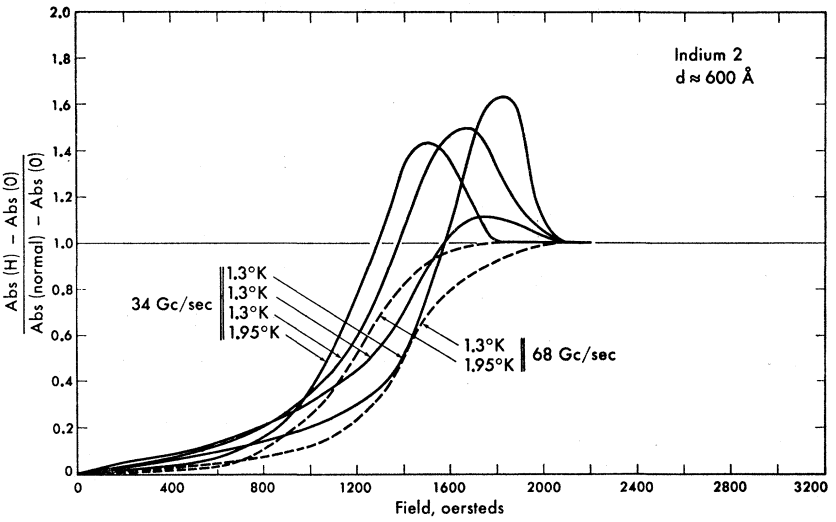

FIG. 7. Anomalous magnetic-field dependence of the absorption in sample indium 2 as a function of frequency and temperature.

perimental points are shown, but instead, only curves which have been smoothed slightly are displayed.

The outstanding feature of these curves is the enhanced absorption, that is, absorption greater than the absorption in the normal state, at some value of H less than the critical field. This enhanced absorption may be observed on all the curves showing absorption at 34 Gc-sec^{-1}, the three curves taken at 1.3°K and the curve taken at 1.95°K. No enhanced absorption is seen in any of the measurements made at 68 Gc-sec^{-1}, however. In fact, the two 68 Gc-sec^{-1} curves are in every way similar to curves obtained on other samples.

It should be noted that the critical field is defined as the field above which the absorption is constant. Thus, on the 34 Gc-sec^{-1} curves showing enhanced absorption the critical field is not where the absorption crosses the line absorption$=1$, but where it returns to this line. This critical field agrees for the three curves of 34 Gc-sec^{-1}, 1.3°K absorption, and is slightly greater than that defined by the 68 Gc-sec^{-1}, 1.3°K curve, as it should be. This is also true of the pair of curves of different frequency taken at 1.95°K. Also, the variation of critical field with temperature is reasonable, as will be seen in the next section.

The three curves taken at 34 Gc-sec^{-1} and 1.3°K were taken on different days with a different orientation of the magnetic field (always approximately parallel to the film). No reasonable explanation of the enhanced absorption or of its variation between runs has been found. Both the enhancement and its variation between runs are well outside of experimental error (about 2%).

An attempt was made to fit these curves assuming that the normal-state conductive σ_n was sufficiently high that the film was no longer thin compared to a wavelength in the normal state. Calculations were made for various assumed values of σ_n using Eq. (A9) of the Appendix, rather than the simplified Eq. (A12). It was found difficult to fit the 34 Gc-sec^{-1} data in this manner and impossible to fit the 68 Gc-sec^{-1} data also, using the same value of σ_n. No further attempt to analyze these data has been made.

IV. ANALYSIS

Parameters of the Samples Determined from Critical-Field Measurements

In this section we determine several parameters which are useful in describing these films. Values of these parameters are inferred from the critical fields found in the parallel and perpendicular orientations. These critical fields are defined by linearly extrapolating the approximately linear portion of the absorption curves to the normal-state absorption. This is done for the 34 Gc-sec^{-1} data for the various experimental conditions of sample and temperature. The 34 Gc-sec^{-1} data are used because the photon energy is fairly small with respect to the gap ($\hbar\omega \leq 2\Delta_0/7$), and these curves will thus be more representative of the low-frequency properties of the superconductor; also, our data are more extensive at this frequency.

From the measurements of the perpendicular critical field $H_{c\perp}(t)$ at a reduced temperature t ($t=T/T_c$), we first calculate $\lambda(0)$, the penetration depth in the film sample at $T=0$, using the relation[10]

$$H_{c\perp}(t)=[4\pi\lambda^2(0)H_{cb}^2(0)/\varphi_0][(1-t^2)/(1+t^2)], \quad (1)$$

where φ_0 is the flux quantum for pairs, $\varphi_0=hc/2e=2.07\times10^{-7}$ G cm^2, and $H_{cb}(0)$ is the critical field for a bulk sample at $T=0$.

Next, we calculate the ratio of the penetration depth to the film thickness $\lambda(0)/d$ using the relation from GL[7]

$$H_{c\parallel}(t)=2(6)^{1/2}H_{cb}(t)\lambda(t)/d, \quad (2)$$

TABLE I. Superconducting parameters of the samples. $H_{c\perp}(t)$ and $H_{c\parallel}(t)$ are measured quantities. $\lambda(0)$, d, and ξ are inferred, using table values for $H_{cb}(0)$, λ_L, and ξ_0.

Sample	t	$H_{c\perp}(t)$	$H_{c\perp}(t)\times\left(\frac{1+t^2}{1-t^2}\right)$	$H_{cb}(0)$[a]	$\lambda(0)$ (Å)	$H_{cb}(t)$[a]	$H_{c\parallel}(t)$	$\lambda(0)/d$	d (Å)	λ_L (Å)	ξ_0 (Å)	ξ (Å)
Indium 2	0.38					232	1475	1.27				
	0.58					181	1275	1.28				
Indium 3	0.38	250	335	269	877	232	7050	6.15	143	350[b]	2600[b]	414
Tin 1	0.35	450	577	305	1011	264	3950	3.04	333	355[c]	2300[c]	283
	0.54	312	566	305	1001	211	3375	3.13	321	355[c]	2300[c]	289
Lead 1	0.18	3000	3220	805	906	782	8025	2.10	432	370[c]	830[c]	138
	0.28	2900	3390	805	930	749	7700	2.09	444	370[c]	830[c]	131
Pb II	0.30	1110	1330	805	583	725	5360	1.50	389	370[c]	830[c]	334
Morris (Ref. 2)	0.64	525	1260	805	567	500	3700	1.38	410	370[c]	830[c]	354

[a] D. Schoenberg, *Superconductivity* (Cambridge University Press, New York, 1952), p. 224, Fig. 77.
[b] A. M. Toxen, Phys. Rev. **127**, 382 (1962).
[c] J. Bardeen and J. R. Schrieffer, in *Progress in Low Temperature Physics*, edited by C. J. Gorter (North-Holland Publishing Company, Amsterdam, 1961), Vol. III.

and the Gorter-Casimir[11] temperature dependence of the penetration depth

$$\lambda(t)=\lambda(0)/(1-t^4)^{1/2}. \tag{3}$$

From this and the above calculation of $\lambda(0)$, we determine the thickness d.

Finally, we determine the coherence length in the film ξ from the approximate relation[12]

$$\lambda=\lambda_L(\xi_0/\xi)^{1/2}, \tag{4}$$

where λ_L is the London penetration depth and ξ_0 is the coherence length in an ideal bulk sample.

Results of these calculations are given in Table I. Since no measurement of $H_{c\perp}$ was made for sample indium 2, complete results cannot be given for this sample. The thickness of samples indium 3, tin 1, and lead 1 used elsewhere in the paper are found by averaging the results for these samples in Table I. The thickness of sample indium 2 is estimated to be 600 Å. The sample Pb II of Morris[2] has been included at the bottom of the table for purposes of comparison. This is the only one of Morris's samples which meets the following two criteria: It is approximately the same thickness as the samples that we have studied, and the perpendicular critical-field measurements were given by Morris.

It is of some interest to compare the values of ξ in the table with the results obtained using the formula[13]

$$1/\xi=1/\xi_0+1/d. \tag{5}$$

This formula gives $\xi=135$ Å for a 145-Å indium film, $\xi=284$ Å for a 325-Å tin film, $\xi=286$ Å for a 435-Å lead film, and $\xi=270$ Å for a 400-Å lead film. Thus, the ξ for our sample indium 3 given in the table seems to be remarkably long, and that for our sample lead 1 is rather short. These descrepancies indicate the inexact nature of the determination. Morris's sample Pb II leads to good agreement between expected and calculated coherence length. Use of Morris's estimate of $d=500$ Å for this film (which is not in agreement with the calculation of d based on his measured $H_{c\perp}$ and $H_{c\parallel}$) would give somewhat better agreement with the ξ determined from his perpendicular critical-field measurements. The excellent agreement between the two methods of determining ξ for our sample tin 1 is presumably fortuitous.

One further comment should be made concerning sample lead 1 and Morris's sample Pb II. The above calculations indicate that λ in lead 1 is much larger than λ in Pb II despite the fact that lead 1 is the thicker sample. This is a reflection of the very high perpendicular critical field found in lead 1 since $H_{c\perp}\sim\lambda^2$ according to Eq. (1). Apparently sample lead 1 is a film with a great deal of additional scattering within the film, which would increase λ and might influence other superconducting properties in the sample. In particular, this short mean free path accounts for the ξ value in Table I being so much smaller than that found using (5), since (5) is based on the assumption that volume scattering is negligible compared to surface scattering.

Method of Determination of an Energy Gap from Absorption Measurements

As was noted above, the theory of Mattis and Bardeen[9] gives formulas for the calculation of the superconducting to normal conductivity ratio $\sigma_s/\sigma_n=(\sigma_1-i\sigma_2)/\sigma_n$ in the extreme anomalous limit. It has been found useful to compare various far-infrared experimental results[14–16] with conductivity ratios and

[11] C. J. Gorter and H. B. G. Casimir, Physik. Z. **35**, 963 (1934); Z. Tech. Phys. **15**, 539 (1934).
[12] A. B. Pippard, Proc. Roy. Soc. (London) **A216**, 547 (1953).
[13] M. Tinkham, Phys. Rev. **110**, 26 (1958).
[14] R. E. Glover, III, and M. Tinkham, Phys. Rev. **108**, 243 (1957).
[15] D. M. Ginsberg and M. Tinkham, Phys. Rev. **118**, 990 (1960).
[16] P. L. Richards and M. Tinkham, Phys. Rev. **119**, 575 (1960).

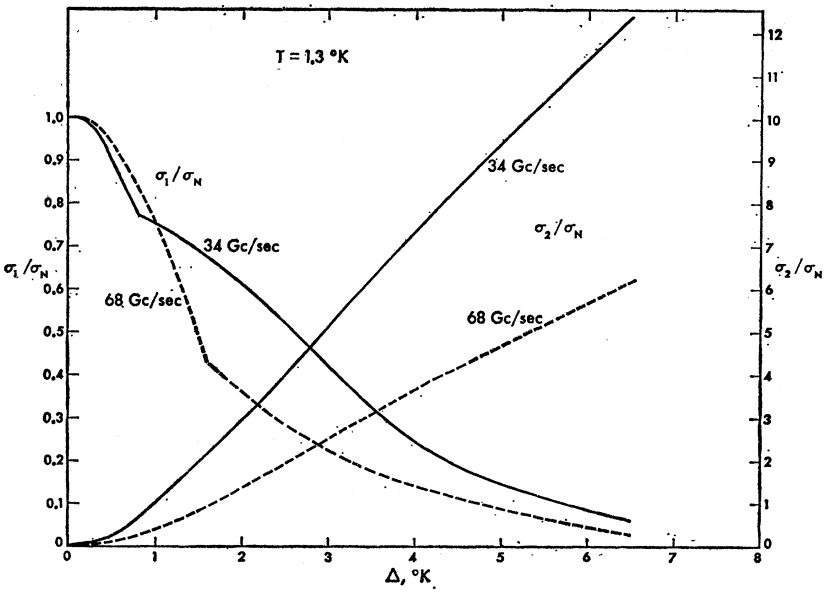

FIG. 8. Theoretical dependence of σ_1/σ_n and σ_2/σ_n on Δ at 34 and 68 Gc/sec and 1.3°K.

surface impedance ratios determined from the formulas of Mattis-Bardeen. Agreement has been generally good, although there are details of the experimental results which are not predicted by the theory. Because of this agreement we make use of calculations based on these formulas.

Extensive calculations based on these formulas of Mattis-Bardeen have been carried out by Miller.[17] Included are calculations of σ_1/σ_n and σ_2/σ_n as functions of $h\nu/kT$ for various values of Δ/kT, where Δ is half the energy gap. From plots of Miller's results we have derived curves of σ_1/σ_n and σ_2/σ_n versus Δ for the various combinations of temperature and frequency relevant to our experiments. As an example, in Fig. 8 we show σ_1/σ_n and σ_2/σ_n plotted versus Δ for $\nu=34$ and 68 Gc/sec and $T=1.3$°K.

The relative absorption, Abs(superconducting)/Abs(normal), is then calculated as a function of Δ using the σ_1/σ_n and σ_2/σ_n from Fig. 8 or from similar curves for the relevant values of temperature and frequency. The relative absorption for the case of a film sufficiently thin that $d \ll \lambda$, but also sufficiently thick

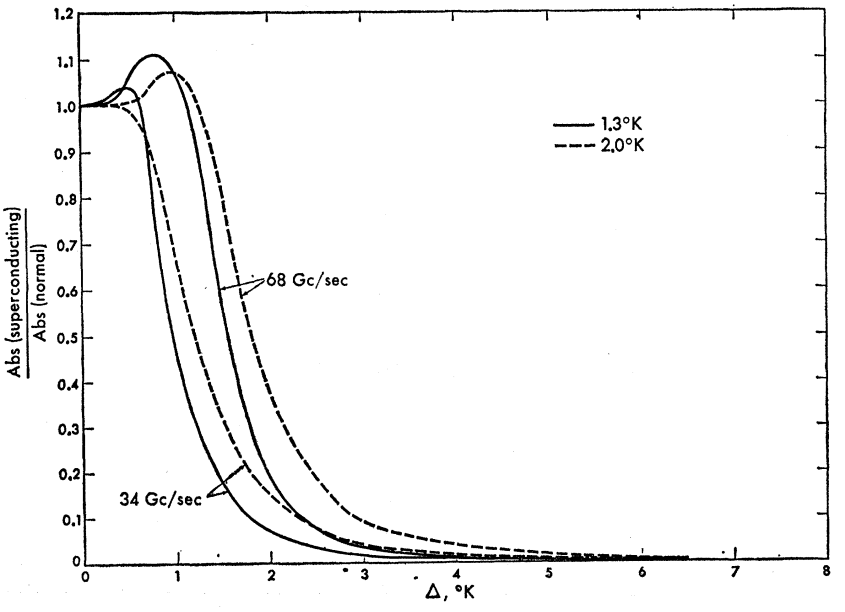

FIG. 9. Calculated absorption versus Δ at 34 and 68 Gc/sec and 1.3 and 2.0°K using Eq. (6).

[17] P. Miller, Phys. Rev. 118, 928 (1960).

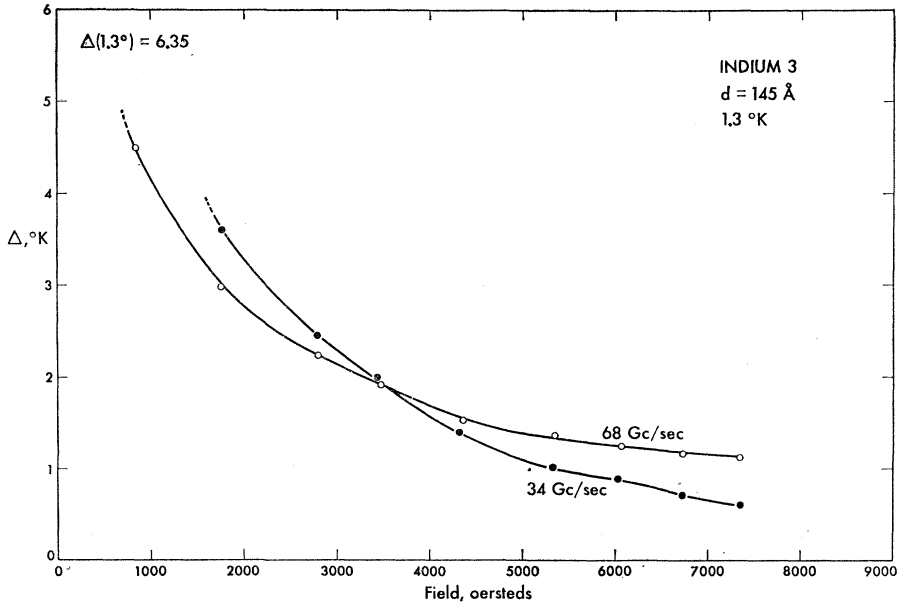

FIG. 10. Magnetic-field dependence of the effective energy gap in sample indium 3 as inferred from the microwave absorption data in Fig. 3.

that the impedance of the film is much less than the impedance of free space, is found to be

$$\frac{\text{Abs (super)}}{\text{Abs (normal)}}=\frac{\sigma_1/\sigma_n}{(\sigma_1/\sigma_n)^2+(\sigma_2/\sigma_n)^2}. \tag{6}$$

This result is obtained in the normal skin effect limit and for normal incidence. The derivation of this formula is outlined in the Appendix. Examples of the relative absorption versus Δ curves found in this way are shown in Fig. 9 for $T=1.3$ and 2.0°K and 34 and 68 Gc-sec^{-1}. From these curves and from our experimental curves of absorption versus H for H parallel to the plane of the sample we finally infer curves of an effective half-energy gap Δ versus H. These curves are discussed in the next section.

Discussion of the Δ Versus H Curves

Curves of Δ versus H derived in the manner described above are shown in Figs. 10–12. These figures show such curves for samples indium 3, tin 1, and lead 1. Values of Δ at $H=0$ have been indicated in these figures. These have been derived from averages of the tunneling results of Giaever and Megerle[4] and of the far-infrared results of Ginsberg and Tinkham[15]

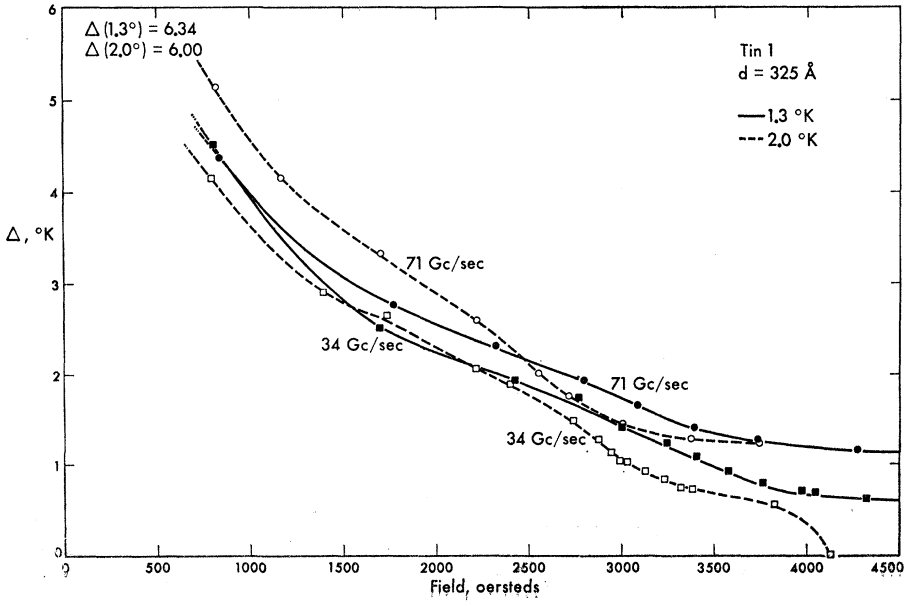

FIG. 11. Magnetic-field dependence of the effective energy gap in sample tin 1 as inferred from the microwave absorption data in Fig. 5.

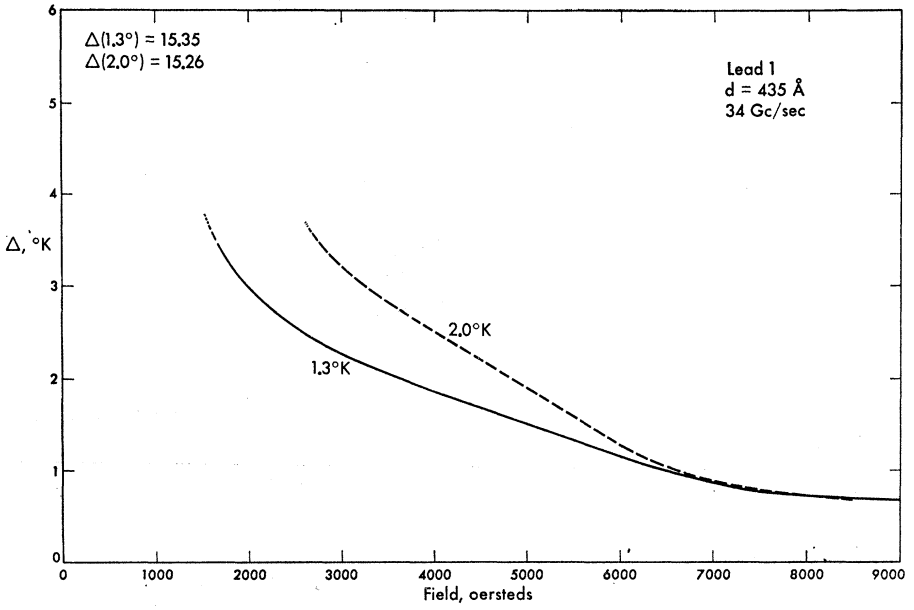

FIG. 12. Magnetic-field dependence of the effective energy gap in sample lead 1 as inferred from the microwave absorption data in Fig. 6.

and of Richards and Tinkham,[16] and they have been corrected to the experimental temperatures. The present experiments are unable to determine a gap parameter for $\Delta > \sim 4°K$ (depending somewhat upon frequency and temperature) since the calculated absorption is then so low as to be lost in the experimental error. The highest field point is the point at which the calculated absorption versus Δ curves cross the line of normalized absorption equal to unity. Since we see no overshoot in the absorption for these samples (as opposed to the anomalous sample indium 2, in which we see far too much overshoot at 34 Gc-sec^{-1}), we are unable to determine any smaller Δ.

It must be noted that the effective gap parameter which we have inferred in this way falls very rapidly as a function of H when compared to other experimental results and with theory. The GL theory,[7] which should be valid near T_c, predicts

$$\Delta/\Delta_0 = (1-h^2)^{1/2}, \tag{7}$$

where $h = H/H_c$. The tunneling experiments of Douglass[5] and of Giaever and Megerle[4] on aluminum indicate such a dependence. Also, Morris's[2] measurements of the thermal conductivity at fairly high reduced temperatures are in fair agreement with this dependence. However, Morris's results at lower reduced temperatures on tin and indium samples fit the dependence

$$\Delta/\Delta_0 = 1-h^2 \tag{8}$$

quite well. Finally, his experiments on lead at low reduced temperatures indicate that the initial decrease of Δ/Δ_0 in a magnetic field is somewhat faster than this. Also, the tunneling experiments of Douglass and Meservey[6] on lead at low reduced temperatures show

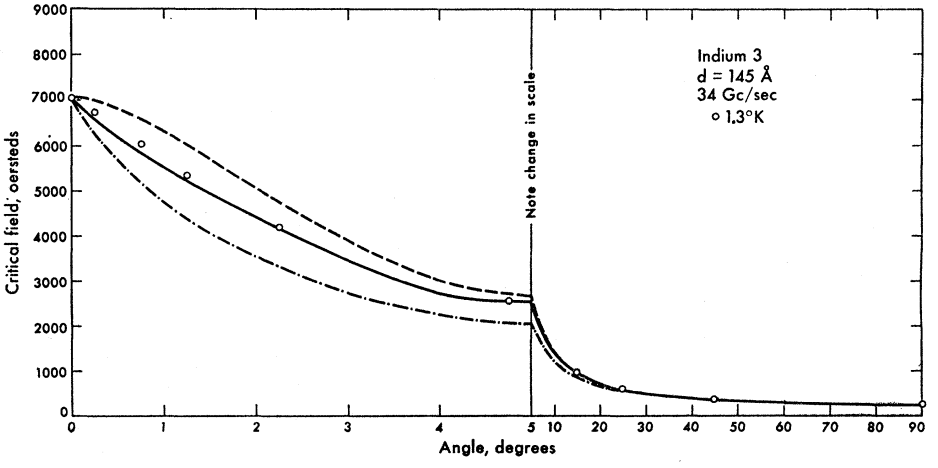

FIG. 13. Angular dependence of the critical field in sample indium 3.

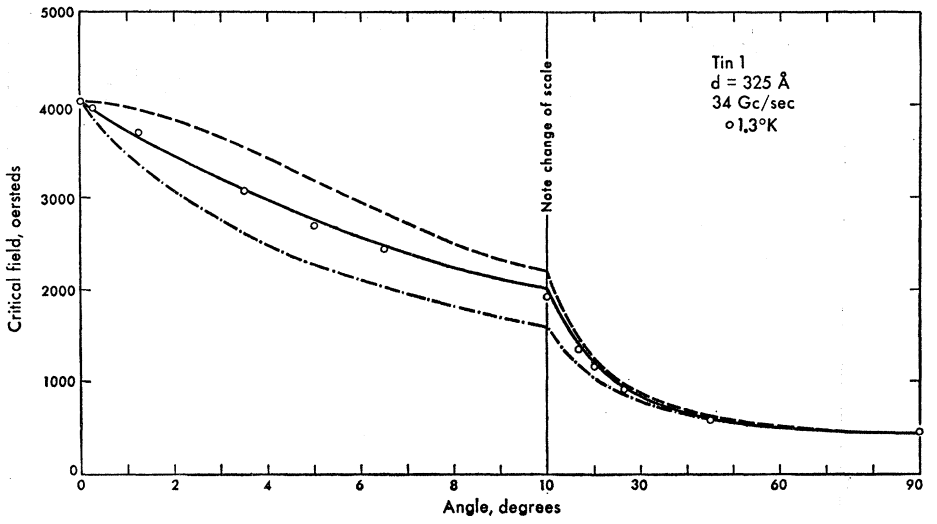

FIG. 14. Angular dependence of the critical field in sample tin 1.

a magnetic-field dependence approximating Eq. (8). The recent theory of Nambu and Tuan[8] fits all these results quite well.

All these magnetic-field dependences show a much slower decrease in Δ than that observed in the present experiments. In Fig. 3 the absorption which would be expected at 34 Gc-sec^{-1} as a function of H from dependences of Δ/Δ_0 of $1-h^2$ and $(1-h^2)^{1/2}$ are shown in the dashed curves. These curves predict much less absorption than was found in our experiments until H is very near H_c, and then the dependence becomes very steep. The qualitative features of such curves are very different from those of the experimental absorption curves reported here.

A possible basis for reconciling the results is offered in the theory of Nambu and Tuan.[8] They indicate that electrons moving parallel to the surface of a film provide a special situation in their theory. Since the magnetic field will tend to confine such an electron and the one with which it is paired to opposite surfaces of the film, Nambu and Tuan conclude that these electrons would be expected to contribute little to the pairing energy of superconductivity. Hence, they will have a small energy gap. It would seem that such electrons would contribute particularly heavily to the absorption of electromagnetic waves incident normally on the film, thus causing more absorption at lower fields and broadening the transition region, as we observe.

It should be pointed out that a misalignment of the field so that the field is not strictly parallel to the film tends to give increased absorption at low fields. Our observation that the linear portion of the absorption curves has about the same slope for all angles seems to preclude this as a complete explanation of the low values of Δ which we find in a magnetic field. Also, the misalignment must have been very small in samples indium 3 and tin 1, since the orientation H parallel to the sample could be found within $\frac{1}{4}$ deg, yet the Δ versus H curves for these samples are very similar to those of other samples.

One should recall from Figs. 3 and 5 that the normalized absorption at 68 or 71 Gc-sec^{-1} is in general higher than that at 34-Gc-sec^{-1}. However, Figs. 10 and 11 show that the $\Delta(H)$ inferred from the higher frequency data is almost always higher than that inferred from the corresponding 34-Gc-sec^{-1} data, particularly at higher fields (smaller reduced gaps) where our determination of Δ is more precise. Thus, the difference between the absorption curves at the two frequencies is not so great as would be expected from the theory of Mattis and Bardeen[9,17] for a superconductor described by a unique effective gap parameter Δ, taken to be a function of H as well as T.

Finally, it should be noted that the Δ versus H curves for sample lead 1 are very similar to those for the tin and indium samples, despite the fact that the energy gap (in zero field) in lead is more than twice that in tin or indium. It would appear that Δ, rather than Δ/Δ_0, is a universal function of H/H_c whenever Δ is small enough for these experiments to be sensitive to it. The unlikeliness of this conclusion casts further doubt on the validity of this analysis in terms of a unique effective gap parameter.

It thus appears that there is a large disagreement between the Δ versus H curves found in these experiments and those found in previous experiments as well as those expected theoretically. Due to this major disagreement and due to the inconsistency among our results at different frequencies it must be concluded that the procedure which we have used above is too naive. A possible conclusion is that under our experimental conditions different groups of electrons have different energy gaps, leading to an averaged absorption which cannot be meaningfully characterized by a single effective gap parameter. In fact, to account for the huge deviations from the behavior expected from

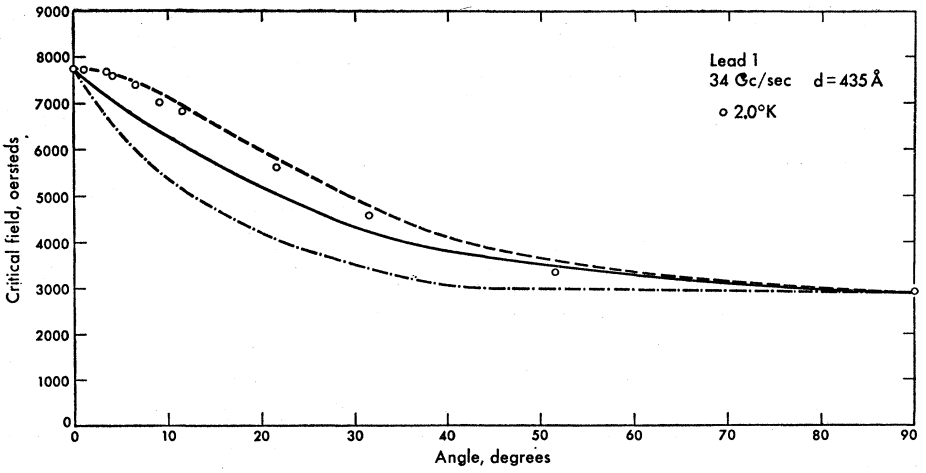

FIG. 15. Angular dependence of the critical field in sample lead 1.

a unique gap it seems likely that a substantial fraction of the electrons must act as though they had essentially no gap at all. Such a possibility is suggested by the theory of Maki,[18] but as no calculation of microwave absorption according to this theory is available, no detailed comparison can be made at present.

Angular Dependence of the Critical Field

Experiments measuring the absorption as a function of angle were carried out for three of our samples, as was noted above. From these measurements we have derived critical field versus angle plots for these three samples, indium 3, tin 1, and lead 1 (see Figs. 13, 14, and 15).

The experimental points are determined by extrapolating the linear portion of the absorption curves taken at 34 Gc-sec^{-1} to the normal-state absorption. Such an extrapolation avoids the difficulty of determining the point where the rounded shoulder of the curve finally reaches the normal-state absorption. In any case, this shoulder is probably related to inhomogeneities in the film and field. Also, the extrapolation should be more representative of the critical field than a definition based on, say, the 50% absorption point. Since the theory of Tinkham[10] is concerned with the value of the critical field, not the approach to this critical field, the extrapolation seems preferable. Fortunately, as noted above, the absorption curves have a linear portion which has a fairly constant slope as a function of angle, so that the angular dependence does not depend critically upon the definition used for the critical field.

Also plotted are three curves which represent calculations of the angular dependence of the critical field. The middle, solid curve is a plot of the formula[10]

$$(H_c \sin\theta/H_{c\perp})+(H_c \cos\theta/H_{c\parallel})^2=1. \quad (9)$$

The lower chain curve is a plot of the formula proposed by Morris[2] to fit his data on his sample Pb II,

$$(H_c \sin\theta/H_{c\perp})+(H_c \cos\theta/H_{c\parallel})=1. \quad (10)$$

The upper, dashed curve has both perpendicular and parallel components entering quadratically,

$$(H_c \sin\theta/H_{c\perp})^2+(H_c \cos\theta/H_{c\parallel})^2=1, \quad (11)$$

as would be expected for a susceptibility which is field-independent to first order.

The experiments on samples indium 3 and tin 1 (Figs. 13 and 14) fit Eq. (9) (solid curve) very well. All the calculated curves have been fitted at the two end points; that is, the parameters $H_{c\perp}$ and $H_{c\parallel}$ appearing in the calculations are the measured critical fields at 0 and 90 deg. In Fig. 13 the experimental points near 0 deg, which are consistently slightly above the solid curve, would fall on it if the angle $\theta=0$ had been incorrectly determined by less than $\frac{1}{4}$ deg. In Fig. 14, the points between 10 and 45 deg appear consistently low when compared to the calculation based on Eq. (9). However, since the curves have been fitted only at the end points, it may be more proper to conclude that we have incorrectly determined the *one* experimental point at 90 deg at too high a value, so that all theoretical curves have been shifted slightly upward from where they should be.

The experiments on sample lead 1 yield different results, however. For this sample the critical field was essentially constant over 1 deg near 0 deg, and the experimental points are best fitted by the upper curve [Eq. (11)]. This result is initially surprising, since, as was noted above, it was Morris's sample Pb II which led him to propose the angular dependence indicated by the chain-line curve [Eq. (10)], and lead 1 and Pb II are of similar thickness (~400 Å). However, lead 1 is apparently a rather poor quality film, with excessive scattering (see the first section under Analysis above) leading to $\xi \approx d/3$, whereas, for Pb II, $\xi \approx d$.

[18] K. Maki, Progr. Theoret. Phys. (Kyoto) 29, 603 (1963), and to be published.

Since the two-dimensional theory leading to Eq. (9) is only expected to be valid if $d \lesssim \xi$, it is reasonable that a discrepancy should occur for the film lead 1, which is thick enough compared to ξ to allow variation in the third dimension. It would be very desirable to clarify the limitations on the applicability of Eq. (9).

V. CONCLUSIONS

Experiments measuring the absorption of 34-Gc-sec^{-1} and 68- or 71-Gc-sec^{-1} microwave radiation in superconducting films have been carried out. This absorption has been measured as a function of magnetic field for film samples of indium, tin, and lead between 145 and 700 Å thick, thin enough so that the superconducting-normal-phase transition is of second order. Experiments have been conducted with H parallel to the film, and also as a function of the angle between the film sample and the field.

The curves of absorption versus H found in these experiments have the following general characteristics:

(a) The portion of the absorption curves between $H=0$ and $H \approx H_c/2$ is approximately quadratic in H, the rise becoming steeper with increasing angle θ between field and film.

(b) The portion of the absorption curves between $H \approx H_c/2$ and H near H_c is approximately linear in H. The slope of this portion of the curve is approximately independent of angle, but this portion of the curve shifts to lower fields as θ is increased.

(c) There is a rounded shoulder of the absorption curve as the absorption approaches the normal-state absorption at H_c. This portion of the absorption curve is shifted to lower fields along with the linear portion as θ is increased, but it is otherwise not significantly changed.

(d) There is no region of absorption significantly greater than the normal-state absorption except for one sample (indium 2). In the case of this sample, there is a region of anomalously high absorption at 34 Gc-sec^{-1}, but no region of absorption greater than the normal state absorption at 68 Gc-sec^{-1}.

Curves of absorption versus the half-energy gap Δ were found from the calculations of Miller,[17] based on the theory of Mattis-Bardeen.[9] From these curves and absorption versus field curves in the parallel field orientation, an effective gap Δ was inferred as a function of H for the various experimental conditions of sample, frequency, and temperature. The field dependence of this effective gap Δ was then compared with previous experiments and with theory.[2-8] It was found that the effective gap which we have inferred decreases much too rapidly as a function of reduced field, for low fields, when our results are compared with previous results and with theory. Also, the effective gap which we have inferred from the higher frequency data (68 or 71 Gc-sec^{-1}) is generally somewhat higher than the one inferred from the 34-Gc-sec^{-1} data. This is a reflection of the fact that although the normalized absorption is greater at the higher frequency than at 34 Gc-sec^{-1}, the difference is not great enough to determine a consistent value of Δ.

Due to the disagreement between these results and previous theory and experiments, as well as the inconsistency within these results, it must be concluded that the above procedure for determining an effective energy-gap parameter as a function of H is too naive. A possible conclusion is that under our experimental conditions different electrons have different energy gaps, so that the spectrum of excitations is quite different in the presence of the field than in the usual BCS superconductor. The absorption which has been observed is then an averaged absorption which cannot be properly characterized by a unique effective gap parameter in the usual BCS framework. Alternatively, inhomogeneities in film thickness leading to a spread in local critical field might account for the observed absorption curves.

In view of the disagreement between the Δ versus H dependences which have been found here and the results of previous experiments, further experiments on electromagnetic properties of superconductors under similar conditions would be very valuable. In particular, since these absorption measurements at 34 and 71 Gc-sec^{-1} are quite insensitive to Δ until Δ has been reduced considerably from the field-free value, measurements at higher frequencies near the field-free gap would be particularly valuable.

The absorption curves taken at 34 Gc-sec^{-1} have also been used to determine the angular dependence of the critical field. The approximately linear portion of these curves has been extrapolated to unity and the critical field thus determined has been plotted as a function of angle. For the films where $d \lesssim \xi$, the angular dependence of the critical field agrees well with Eq. (9), presented previously.[10]

APPENDIX: CALCULATION OF THE ABSORPTION IN A THIN FILM

A formula for the ratio of the absorption in the superconducting state to the absorption in the normal state, Abs(super)/Abs(normal), is determined here subject to certain simplifying assumptions. The absorption ratio is found for a plane wave at normal incidence to a plane film of thickness d bounded by free space. The effect of non-normal incidence on the absorption ratio should be small, and the effect of the substrate should be very small as long as the substrate is much less than a wavelength thick and the impedance of the substrate is much closer to the impedance of free space than to the impedance of the film sample. The impedance of the nonresonant cavity is very near to that of free space for the frequencies of interest in these experi-

ments. The calculation is done in the local limit (normal skin effect).

Consider a plane wave of unit amplitude in the z direction incident upon a film of thickness d with refractive index $\bar{n}=n(1-ik)$. At the first surface at $z=0$, there will be the incident wave; a reflected wave, R_0; a transmitted wave, T_1; and a wave reflected from the second surface, $R_1\exp[-2\pi i\bar{n}d/\lambda]$, where λ is the free space wavelength. At the second surface at $z=d$, there is the first transmitted wave, $T_1\exp[-2\pi i\bar{n}d/\lambda]$; the wave reflected at this boundary, R_1; and a transmitted wave, T_2. From matching boundary conditions we find the following four equations:

$$1+R_0=T_1+R_1e^{-2\pi i\bar{n}d/\lambda}, \tag{A1}$$

$$1-R_0=\bar{n}(T_1-R_1e^{-2\pi i\bar{n}d/\lambda}), \tag{A2}$$

$$T_1e^{-2\pi i\bar{n}d/\lambda}+R_1=T_2, \tag{A3}$$

$$\bar{n}(T_1e^{-2\pi i\bar{n}d/\lambda}-R_1)=T_2. \tag{A4}$$

These can be solved for the four amplitudes R_0, T_1, R_1, and T_2 relative to the unit input amplitude.

To calculate the power absorbed in the sample, however, we are only interested in the difference between the input power and the sum of the output powers, which is

$$\text{Abs.}=1-|R_0|^2-|T_2|^2. \tag{A5}$$

This may be calculated in terms of $\bar{n}=n-ink$. For metal films it is more convenient to transform to the complex conductivity $\bar{\sigma}=\sigma_1-i\sigma_2$. Then we have

$$\bar{n}^2=\bar{\epsilon}=\sigma_2/\epsilon_0\omega-i\sigma_1/\epsilon_0\omega, \tag{A6}$$

and we find

$$n=\{[(\sigma_1^2+\sigma_2^2)^{1/2}+\sigma_2]/2\epsilon_0\omega\}^{1/2}; \tag{A7}$$

$$nk=\{[(\sigma_1^2+\sigma_2^2)^{1/2}-\sigma_2]/2\epsilon_0\omega\}^{1/2}. \tag{A8}$$

If we also introduce the parameters x and x',

$$x=4\pi nd/\lambda;\quad x'=4\pi nkd/\lambda,$$

then we finally find a formula for the absorptivity of a film which is in fairly simple form

Absorptivity

$$\begin{aligned}=&[(4/\epsilon_0\omega)\{[(\sigma_1^2+\sigma_2^2)^{1/2}+\sigma_2]\cosh x'\\&+[(\sigma_1^2+\sigma_2^2)^{1/2}-\sigma_2]\cos x-2(\sigma_1^2+\sigma_2^2)^{1/2}\}\\&+[4(\sigma_1^2+\sigma_2^2)^{1/2}/\epsilon_0\omega][n\sinh x'+nk\sin x]\\&+4[n\sinh x'-nk\sin x]]\\&\times[[(\sigma_1^2+\sigma_2^2)/\epsilon_0^2\omega^2+2\sigma_2/\epsilon_0\omega+1][\cosh x'-\cos x]\\&+[4(\sigma_1^2+\sigma_2^2)^{1/2}/\epsilon_0\omega][\cosh x'+\cos x+n\sinh x'\\&\qquad+nk\sin x]+4[n\sinh x'-nk\sin x]]^{-1}.\end{aligned} \tag{A9}$$

Let us take the limit where the arguments x and x' of the trigonometric and hyperbolic functions are small, and take only the leading terms in the power series expansion, thus neglecting terms of order $(4\pi d/\lambda)^2\times(\sigma/\epsilon_0\omega)$ compared with unity. We also neglect terms of order $(d/\lambda)^2$ compared to unity, but we retain terms in $(d/\lambda)(\sigma/\epsilon_0\omega)$ and $(d/\lambda)^2\times(\sigma/\epsilon_0\omega)^2$, which are not necessarily small compared to unity unless the film is very thin.

In this approximation we find a greatly simplified formula for the absorption:

Absorptivity

$$=\frac{(\sigma_1/\epsilon_0\omega)(4\pi d/\lambda)}{2+(\sigma_1/\epsilon_0\omega)(4\pi d/\lambda)+\frac{1}{8}[(\sigma_1^2+\sigma_2^2)/\epsilon_0^2\omega^2][4\pi d/\lambda]^2}, \tag{A10}$$

which is valid when x and x' are much less than unity. If we note that for our films of the order of a few hundred angstroms thickness the impedance of the film is much less than that of free space, we see that we need keep only the final term in the denominator. Thus, we find

$$\text{Absorptivity}=(2\epsilon_0\omega\lambda/\pi d)\times[\sigma_1/(\sigma_1^2+\sigma_2^2)]. \tag{A11}$$

Finally, to get the absorptivity ratio this is divided by the corresponding normal state absorptivity, yielding

$$\frac{\text{Abs (super)}}{\text{Abs (normal)}}=\frac{\sigma_1/\sigma_n}{(\sigma_1/\sigma_n)^2+(\sigma_2/\sigma_n)^2}. \tag{A12}$$

This is the formula used to interpret the experimental results. It may also be derived in an elementary way by treating the film as infinitely thin, but this simpler derivation would give no information about its range of applicability.